2019

Exfoliation of scalable few layer biocompatible graphene nanosheets using a protein-assisted mechano-chemical technique

Deepak-George Thomas
Iowa State University

Exfoliation of scalable few layer biocompatible graphene nanosheets using a protein-assisted mechano-chemical technique

by

Deepak-George Thomas

A thesis submitted to the graduate faculty

in partial fulfillment of the requirements for the degree of

MASTER OF SCIENCE

Major: Mechanical Engineering

Program of Study Committee:
Nicole Nastaran Hashemi, Major Professor
Emily Smith
Reza Montazami

The student author, whose presentation of the scholarship herein was approved by the program of study committee, is solely responsible for the content of this thesis. The Graduate College will ensure this thesis is globally accessible and will not permit alterations after a degree is conferred.

Iowa State University

Ames, Iowa

2019

DEDICATION

I humbly dedicate this thesis to my parents and sister. I am grateful for being given the resources to pursue my education and for the unwavering belief you always had in me.

TABLE OF CONTENTS

Page

LIST OF FIGURES

Page

ACKNOWLEDGMENTS

I would like to express my gratitude to my committee chair, Nicole Nastaran Hashemi, and my committee members, Dr. Reza Montazami and Dr. Emily Smith for assisting me in my research.

Additionally, I am thankful to Dr. Shalabh Gupta for giving me access to his chemical inventory and guiding me during my project.

Furthermore, I wish to extend my appreciation to the Department of Mechanical Engineering for providing me with an excellent education and a cherishable experience.

ABSTRACT

The ubiquitous applications in which graphene plays an integral role has made it essential to develop a facile, cheap, environmentally-friendly and scalable manufacturing technique, that can meet its ever-growing demand. This thesis investigates a mechano-chemical method to exfoliate Few-Layered Graphene (FLG) dispersions. A common protein, Bovine Serum Albumin (BSA) is implemented that has been found to improve the effectiveness of the exfoliation process as well as prevent graphene layers from aggregating back after it has been separated. Moreover, Astrocytes cells were brought in contact with the developed BSA-FLG dispersions in order to test for cell cytotoxicity as a part of a preliminary study. The results indicate that cells thrived when subjected to BSA-FLG dispersions up until a certain concentration. In addition, an exhaustive literature review on existing ball milling techniques used to synthesize graphene has been included.

CHAPTER 1. INTRODUCTION

1.1 Overview

The fascinating properties of graphene has enabled researchers to derive diverse applications from it. A few of its properties are described below –

1. High Electron-Hole Mobility

Graphene possesses band structure that is symmetric in nature, leading to elevated electron mobility relative to III-V compound semiconductors [1], [2]. Additionally, graphene electron maintain a distinct chirality, which provides them increased mobility by averting intervalley backscattering[3]. This has led scientists to believe that pristine graphene has resistivity in the range of 10^{-6} ohm-cm[4], [5] .

2. Transparency

Graphene absorbs 2.3% of the light over the visible spectra, making it transparent. Its conical band structure close to the Dirac points contributes to its optical properties [5], [6].

3. Substantial Surface Area

Pristine graphene has a surface area equaling 2630 m^2g^{-1} because all of its atoms are in contact with the surface, causing it to have a specific surface that is larger than most materials [7], [5].

Since its isolation in 2004, by Novoselov *et al,* multiple processes have been developed to manufacture graphene. A few of the major methods that has been used by industry as well as the research community is described below –

1. Micromechanical Exfoliation

One of the earliest techniques developed to exfoliate graphene involved splitting graphene layers from graphite using scotch tape and its subsequent acid dissolution leading to the isolation of single layered graphene sheets [8], [9], [10], [11]. This technique, despite producing high quality graphene, can only be used for research purposes due to low yield making it commercially infeasible [12].

2. Liquid Phase Exfoliation

This facile technique involves using surface-active organic fluids that penetrate between the layers of crystalline graphite. The resulting increase in the distance between the graphene layers reduces their corresponding interaction energy. This facilitates exfoliation once mechanical force is applied on them [13].

3. Graphite Oxide Reduction

One of the most common techniques investigated to fabricate graphene is exfoliating graphite oxide into graphene oxide (GO). The motivation behind this process is that it is relatively easier to exfoliate graphite oxide compared to graphite. Numerous processes have been developed to reduce GO into graphene. However, the hydrophilicity of the GO sheet weakens during reduction, causing it to precipitate[14]. Subsequently, the reduction process is never complete and the resulting product is generally referred to as ‘reduced graphene oxide’ (rGO) or ‘functionalized graphene’. The properties of rGO aren’t likely to be equal to that of graphene, even under a state of total reduction, since the oxidation process occurs under severe conditions generating a large number of defects [12].

4. Chemical Vapor Deposition

Chemical Vapor Deposition (CVD) involves the use of transition metal substrates to develop graphene films, via pyrolysis of carbon consisting gases at elevated temperatures. This process can be further subdivided into segregation based and surface-catalysed based. In the former method, the dissolved carbon present within the bulk metal diffuses to the metallic surface. This usually occurs during the cooling process as there is a decrease in the carbon solubility with temperature. The latter method involves the decomposition of materials consisting of carbon on the surface of the metal leading to the development of graphene [15], [16]. This technique allows effortless fabrication of large-area graphene films, however it suffers from the drawback that an extreme environment is required for growing graphene, particularly in cases where ultra-high vacuum is used [17], [12]

5. Epitaxial Growth

This technique involves growing graphene on silicon carbide (SiC) at elevated temperatures (> 1000 °C) while subliming the silicon on the surface. The carbon undergoes a microstructural change via the graphitization process [18]. Graphene of superior quality can be developed using technique, with the application of greater temperatures. A major drawback of this procedure is that SiC is expensive, affecting commercial production [12].

1.2 Research Motivation

There have been numerous advances towards the manufacturing of graphene for commercial purposes, however the conventional techniques in place are usually environmentally hazardous and possess toxic effects [19], [20] , [21], [22]. Lately, there has been a paradigm shift in fabrication processes, focusing on alternate techniques to devise a ‘green

route' to fabricate graphene. Furthermore, the advantageous properties of eco-friendly graphene can be then implemented in biological applications [23], [24]. Guo *et al.* developed a green electrochemical technique to fabricate graphene by reducing exfoliated graphite oxide (GO) [25]. Zhu *et al.* and Gurunathan *et al.* produced graphene by reducing exfoliated GO using glucose and triethylamine respectively [22], [26]. Shams *et al.* produced graphene from camphor leaves by subjecting it to pyrolysis, followed by sonication in presence of trichloromethane and D-Tyrosine. The final step of their environmentally friendly procedure consisted of centrifugation, wherein few layer graphene (FLG) was separated from other carbon compounds [27]. Yi *et al.* produced graphene by sonicating it in water and alcohol and subsequently centrifugation [28].

The following chapters describe a mechano-chemical technique to exfoliate few layer graphene nanosheets in an aqueous dispersion. The process is aided by a commonly found protein, known as Bovine Serum Albumin (BSA).

1.3 References

1. Del Alamo, J. A., Nanometre-scale electronics with III–V compound semiconductors. *Nature* **2011,** *479* (7373), 317.

2. Hwang, E. H.; Sarma, S. D., Acoustic phonon scattering limited carrier mobility in two-dimensional extrinsic graphene. *Physical Review B* **2008,** *77* (11), 115449.

3. Bolotin, K. I.; Sikes, K. J.; Jiang, Z.; Klima, M.; Fudenberg, G.; Hone, J.; Kim, P.; Stormer, H. L., Ultrahigh electron mobility in suspended graphene. *Solid State Communications* **2008,** *146* (9), 351-355.

4. Chen, J.-H.; Jang, C.; Xiao, S.; Ishigami, M.; Fuhrer, M. S., Intrinsic and extrinsic performance limits of graphene devices on SiO 2. *Nature nanotechnology* **2008,** *3* (4), 206.

5. Wang, X.; Shi, Y., Fabrication techniques of graphene nanostructures. **2014**.

6. Nair, R. R.; Blake, P.; Grigorenko, A. N.; Novoselov, K. S.; Booth, T. J.; Stauber, T.; Peres, N. M. R.; Geim, A. K., Fine structure constant defines visual transparency of graphene. *Science* **2008,** *320* (5881), 1308-1308.

7. Schedin, F.; Geim, A. K.; Morozov, S. V.; Hill, E. W.; Blake, P.; Katsnelson, M. I.; Novoselov, K. S., Detection of individual gas molecules adsorbed on graphene. *Nature materials* **2007,** *6* (9), 652.

8. Novoselov, K. S.; Geim, A. K.; Morozov, S. V.; Jiang, D.; Zhang, Y.; Dubonos, S. V.; Grigorieva, I. V.; Firsov, A. A., Electric Field Effect in Atomically Thin Carbon Films. *Science* **2004,** *306* (5696), 666-669.

9. Novoselov, K. S., KS Novoselov, D. Jiang, F. Schedin, TJ Booth, VV Khotkevich, SV Morozov, and AK Geim, Proc. Natl. Acad. Sci. USA 102, 10451 (2005). *Proc. Natl. Acad. Sci. USA* **2005,** *102*, 10451.

10. Novoselov, K. S.; Geim, A. K.; Morozov, S. V.; Jiang, D.; Katsnelson, M. I.; Grigorieva, I. V.; Dubonos, S. V.; Firsov, A. A., Two-dimensional gas of massless Dirac fermions in graphene. *Nature* **2005,** *438*, 197.

11. Geim, A. K.; Novoselov, K. S., The rise of graphene. *Nature Materials* **2007,** *6*, 183.

12. Edwards, R. S.; Coleman, K. S., Graphene synthesis: relationship to applications. *Nanoscale* **2013,** *5* (1), 38-51.

13. Dresselhaus, M. S., MS Dresselhaus and G. Dresselhaus, Adv. Phys. 30, 139 (1981). *Adv. Phys.* **1981,** *30*, 139.

14. Pei, S.; Cheng, H.-M., The reduction of graphene oxide. *Carbon* **2012,** *50* (9), 3210-3228.

15. Wintterlin, J.; Bocquet, M. L., Graphene on metal surfaces. *Surface Science* **2009,** *603* (10-12), 1841-1852.

16. Batzill, M., The surface science of graphene: Metal interfaces, CVD synthesis, nanoribbons, chemical modifications, and defects. *Surface Science Reports* **2012,** *67* (3), 83-115.

17. Li, X.; Cai, W.; An, J.; Kim, S.; Nah, J.; Yang, D.; Piner, R.; Velamakanni, A.; Jung, I.; Tutuc, E., Large-area synthesis of high-quality and uniform graphene films on copper foils. *science* **2009,** *324* (5932), 1312-1314.

18. Sutter, P., Epitaxial graphene: How silicon leaves the scene. *Nature materials* **2009,** *8* (3), 171.

19. Barwich, S.; Khan, U.; Coleman, J. N., A technique to pretreat graphite which allows the rapid dispersion of defect-free graphene in solvents at high concentration. *The Journal of Physical Chemistry C* **2013,** *117* (37), 19212-19218.

20. Gambhir, S.; Murray, E.; Sayyar, S.; Wallace, G. G.; Officer, D. L., Anhydrous organic dispersions of highly reduced chemically converted graphene. *Carbon* **2014,** *76*, 368-377.

21. Hernandez, Y.; Nicolosi, V.; Lotya, M.; Blighe, F. M.; Sun, Z.; De, S.; McGovern, I. T.; Holland, B.; Byrne, M.; Gun'Ko, Y. K., High-yield production of graphene by liquid-phase exfoliation of graphite. *Nature nanotechnology* **2008,** *3* (9), 563.

22. Zhu, C.; Guo, S.; Fang, Y.; Dong, S., Reducing sugar: new functional molecules for the green synthesis of graphene nanosheets. *ACS nano* **2010,** *4* (4), 2429-2437.

23. Novoselov, K. S.; Fal, V. I.; Colombo, L.; Gellert, P. R.; Schwab, M. G.; Kim, K., A roadmap for graphene. *nature* **2012,** *490* (7419), 192.

24. Ahadian, S.; Estili, M.; Surya, V. J.; Ramón-Azcón, J.; Liang, X.; Shiku, H.; Ramalingam, M.; Matsue, T.; Sakka, Y.; Bae, H., Facile and green production of aqueous graphene dispersions for biomedical applications. *Nanoscale* **2015,** *7* (15), 6436-6443.

25. Guo, H.-L.; Wang, X.-F.; Qian, Q.-Y.; Wang, F.-B.; Xia, X.-H., A green approach to the synthesis of graphene nanosheets. *ACS nano* **2009,** *3* (9), 2653-2659.

26. Gurunathan, S.; Han, J. W.; Eppakayala, V.; Kim, J.-H., Microbial reduction of graphene oxide by Escherichia coli: a green chemistry approach. *Colloids and Surfaces B: Biointerfaces* **2013,** *102*, 772-777.

27. Shams, S. S.; Zhang, L. S.; Hu, R.; Zhang, R.; Zhu, J., Synthesis of graphene from biomass: a green chemistry approach. *Materials Letters* **2015,** *161*, 476-479.

28. Yi, M.; Shen, Z.; Ma, S.; Zhang, X., A mixed-solvent strategy for facile and green preparation of graphene by liquid-phase exfoliation of graphite. *Journal of Nanoparticle Research* **2012,** *14* (8), 1003.

CHAPTER 2. PROTEIN ASSISTED MECHANOCHEMICAL EXFOLIATION OF SCALABLE FEW LAYER BIOCOMPATIBLE GRAPHENE NANOSHEETS

Modified from a manuscript to be submitted to RSC Advances

Deepak-George Thomas[a], Steven De-Alwis[a], Shalabh Gupta[b]*, Vitalij K. Pecharsky[b,c], Deyny Mendivelso-Perez[b,d], Emily A. Smith[b,d], Reza Montazami[a], Nicole N. Hashemi[a,e]*

[a] Department of Mechanical Engineering, Iowa State University, Ames, IA, 50011-2030, USA

[b] The Ames Laboratory, U.S Department of Energy, Ames, IA, 50011-3020, USA

[c] Department of Material Science and Engineering, Iowa State University, Ames, IA, 50011-1096, USA

[d] Department of Chemistry, Iowa State University, Ames, IA, 50011-1021, USA

[e] Department of Biomedical Sciences, Iowa State University, Ames, IA 50011, USA

* nastaran@iastate.edu

2.1 Abstract

A facile method to produce few-layer graphene nanosheets is developed using protein-assisted mechanical exfoliation. The predominant shear forces, generated in a planetary ball mill facilitates exfoliation of graphene layers from graphite flakes. The process employs a commonly known protein, Bovine Serum Albumin (BSA), which not only acts as an effective exfoliation agent but also provide stability by preventing restacking of the graphene layers. The latter is demonstrated by the excellent long-term dispersibility of exfoliated graphene in an aqueous BSA solution, which exemplifies a common biological medium. Development of

such potentially scalable and toxin-free methods are critical for producing cost-effective biocompatible graphene, enabling numerous possible biomedical and biological applications. The fabricated product has been characterized using Raman Spectroscopy, powder X-Ray diffraction, Transmission Electron Microscopy and Scanning Electron Microscopy. The BSA-FLG dispersion was then placed in media containing Astrocyte cells to check for cytotoxicity. It was found that lower concentrations of BSA-FLG dispersion had only minute cytotoxic effects on the Astrocyte cells.

2.2 Introduction

Pristine graphene is a two-dimensional material consisting of carbon atoms, hexagonally arranged, exhibiting sp^2 hybridization and forming a sheet possessing the thickness of a single atom [1], [2].

Graphene possesses remarkable electrical, mechanical and thermal properties, attributed to its pi-conjugation [1], [3], [4]. The charge carrier mobility of freely suspended graphene exceeds 2000 $cm^2V^{-1}s^{-1}$ [5], accredited to graphene's outstanding electrical properties [6]. Despite being the thinnest material present, it has a Young's Modulus of approximately 1 TPa making it stronger than steel [7], [8]. A variety of fields including biology and medicine have begun tapping into the immense potential that graphene presents. He *et al.* used graphene as a surface enhanced Raman scattering (SERS) substrate in order to carry out multiplex DNA detection [9]. Rastogi *et al.* discovered that cell adhesion and proliferation for neuronal and non-neuronal cells was enhanced by the use of single layer graphene [10].

Many methods have been developed to fabricate graphene since the last decade. The prominent ones can be broadly classified into - i) Epitaxial growth of graphene [11], ii)

Micromechanical exfoliation [12], iii) Exfoliation using Electrochemical Methods [13], iv) Exfoliation using solvents [14] and v) Chemical Vapor Deposition [15]. The fabrication of single layer graphene is difficult and often requires expensive equipment. However, it has been observed that few-layer graphene possesses certain properties that are similar to monolayer graphene such as, the absence of gap in its band structure [16] and its high surface area [17]. Due to these similarities, FLGs can substitute for single layer graphene in various applications, generating cost effective solutions.

Exfoliation using mechanical methods has generally helped develop high quality graphene. Nevertheless, there is still a lot of work to be done in order to improve the efficiency of the process [1]. The exfoliation of graphene layers from bulk graphite is dependent on the Van Der Waals forces between individual graphene layers being overcome through various means. Mechanical methods to curb these forces can be implemented through the application of shear or normal forces [18], [19] leading to the graphite/graphene flakes being broken into smaller sizes. Although smaller flakes possess weaker Van der Waal forces, it prevents acquiring graphene sheets with large surface area [20].

Highly Ordered Pyrolytic Graphite was used to produce graphene via micromechanical cleavage [21], [19], [22]. Normal force was applied on the surface of HOPG using scotch tape and after many iterations single layer graphene was produced. This procedure led to the discovery of mono layer graphene [18]. However, this technique can only be used to produce graphene in minute quantities[18]. Hernandez *et al.* produced graphene by sonicating graphite in organic solvents including N-N-dimethylformamide (DMF) and N-methylpyrrolidone (NMP) and the material was centrifuged after sonication. The limitation of this facile technique was that the graphene yield obtained turned out to be merely 0.01 mg mL^{-1} [14]. Additionally, sonication

works through the principle of cavitation assisting exfoliation leading to excessive local heat generation which causes the material being sonicated to be subjected to enormous pressure and sharp temperature changes [23], [24], [25] making it infeasible for industrial applications.

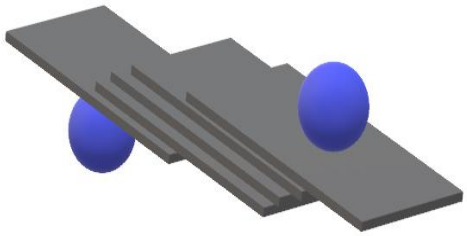

Figure 2-1 Shear exfoliation of graphene layers

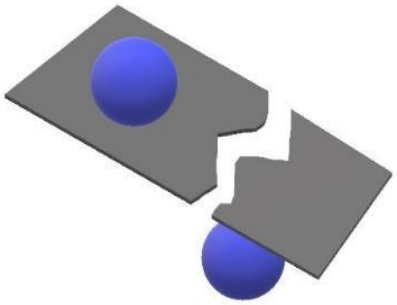

Figure 2-2 Destruction of graphene planes due to normal impact

The principle behind fabrication of graphene using ball milling is that the application of shear force on graphite by the milling balls leads to its exfoliation [Figure 2-1 & 2-2]. This method yields graphene flakes of large size. However, during the milling process, it is probable that the balls may vertically strike the graphite/graphene flakes causing them to reduce in

dimension. Moreover, the crystal structure may also be adversely affected leading to the formation of amorphous material [20]. The ball milling apparatus usually employed to exfoliate graphite are stirred media mills [20] and planetary ball mills [26]. Stirring media mill enables better control of the heat generated during milling. Planetary ball mills simultaneously assist in functionalizing and exfoliating the material being milled due to the application of high energy during operation. The downside of this process is that it is time consuming and despite that the material might require sonication [26].

Chen *et al.* produced hydrophilic graphene dispersions by ball milling graphite for 4 hours at 400 rpm along with poly (vinylpyrrolidone) and supercritical CO_2, using a stirring ball-milling machine [27]. Supercritical materials are maintained above its critical pressure and temperature and have the ability to infiltrate gaseous substances and dissolve liquid substances [28]. CO_2 greatly assists in intercalation for it possesses a molecule size of 0.33 nm, comparable to the graphene interlayer distance of 0.34nm [29]. Furthermore, CO_2 requires relatively low pressure and temperature to reach critical point [28]. Similarly, Zhu *et al.* produced graphene by ball milling graphite with dry ice (solid CO_2) in a planetary mill for 24 hours. The resulting powder was sonicated for 20 minutes in the presence of 1M aqueous HCl solution leading to the formation of edge-carboxylated graphene (ECG). Thermally reduced graphene (TRG) was obtained by annealing the ECG at a temperature of 900º C for a time duration of 10 minutes [30]. Al-Sherbini *et al.* exfoliated graphene using 2-ethylhexanol and kerosene as solvents. A planetary ball mill was employed to conduct the high energy milling operation for a duration of 60 hours at 400 rpm. Centrifugation along with heat treatment was performed in the presence of Argon at 600° C [31]. These techniques although effective in exfoliating graphite, consisted of multiple steps. Zhao et al. conducted ball milling to exfoliate multi-layer graphite nano-

sheets into graphene. The solvent used was N, N - dimethylformamide (DMF) [32]. In this process, the graphitic material was already very thin, with thickness ranging between 30 - 80 nm. Additionally, N, N - dimethylformamide (DMF) has been found to be very hazardous to living organisms [33]. Leon *et al.* developed few layer graphene by milling graphite along with melamine using a planetary ball mill. The parameters for the graphene samples produced, speed of rotation and milling time, ranged between 100 - 250 rpm and 30 - 60 min respectively. The experiments conducted were either in the presence of nitrogen or normal atmosphere [34]. Although a facile procedure was presented, the quantity of input material equaling 30 mg was relatively low.

Lately, the influence of biological materials as exfoliates has also been investigated. Gonzalez *et al.* milled graphite at 250 rpm in the presence of carbohydrate to produce graphene dispersions. They found that glucose showed the highest efficacy in exfoliating graphene with reduced presence of defects [35]. Ahadian *et al.* developed graphene dispersions by sonicating graphite in Bovine Serum Albumin (BSA) media [36]. Bovine Serum Albumin is a protein that is obtained from cows through natural means. BSA possesses both hydrophobic as well as hydrophilic sections. The hydrophobic section is adsorbed on graphene, which also is hydrophobic. This assists in the formation of dispersions and potentially prevents restacking of graphene [36]. Pattammatel *et al.* produced graphene using a kitchen blender after applying shear/turbulence force on graphite in the presence of BSA. They also explored the relation between varying BSA/graphite ratios on the exfoliation rate and came to the conclusion that the best results could be obtained from a ratio of 0.03 [37].

This paper describes a green one-step technique to fabricate bio-compatible graphene using a planetary ball mill. One of the objectives of this experimental study was to investigate

techniques to facilitate the fabrication of mass produced graphene, therefore the aqueous dispersion of FLG produced is not centrifuged after it has been collected. Moreover, to utilize the beneficial effects that BSA lends to FLG's biocompatibility, these two materials are not separated in any post-processing step.

2.3 Materials and Method

Bovine Serum Albumin (CAS: 9048-46-8) and Graphite were purchased from Sigma Aldrich USA. The concentration of graphite was kept constant throughout the study equal to 100 mg. The concentration of BSA was varied according to the design of the experiment. In addition, 5 mL of water was added to the graphite-BSA mixture to prepare a solution. A horizontal planetary milling containing two stations (Fritsch, Pulverisette 7) was used for the mechano-chemical milling process. The milling containers were made of 316L grade stainless steel. They also possessed a lining composed of 440C-hardened stainless steel, which protected it from wear and the experimental samples from contamination. The speed of rotation was kept constant at 300 rpm, with the milling jars being kept at room temperature. The direction of rotation alternated along with intermittent pauses to prevent overheating. Sixteen chrome steel balls (AISI E52100, ρ~7.83 g cm^{-3}), possessing a weight of 8.3g were placed in each of the steel jars.

2.4 Results and Discussion

Figure 2-3 Smooth graphene solution produced after milling BSA and graphite in the ratio of 1:10

Figure 2-4 Foamy graphene solution produced after milling BSA and graphite at ratios of 1:2 and above

The texture of the fluid recovered after ball milling varied depending upon the amount of BSA present. FLG fluids in the presence of minute quantities of BSA *(≤10%)* had smooth textures. Whereas FLG that was exfoliated in the presence of large amounts of BSA *(≥50%)* displayed a foamy texture and usually had to be scooped out using a spatula [Figure 2-3 & 2-4]. Additionally, the dispersions with large concentrations of BSA were found to disperse for several days

2.4.1 Effect of BSA on the exfoliation of graphene

Ahadian *et al.* established the molecular interaction occurring between BSA and graphene under the assumption that there is no interplay between graphene and the hydrophilic amino acid portion of BSA. In order to better understand the underlying process, density functional theory (DFT) calculations of the charge transfer, binding energy and density of states (DOS) analyses were performed by them. The impact of individual amino acids in the exfoliation of graphene sheets was discerned by calculating the product of the number of amino acids with their respective binding energy values. The impact of the amino acids in descending order is, Leu, Pro, Ala, Cys, Val, Phe, Tyr, Gly, ILeu, Met, Tyrp . The charge transfer calculations helped determine that the removal of electrons from graphene was due to the effect of electronegative atoms from amino acid types such as imino, aliphatic and those possessing Sulphur. The interaction between graphene and aromatic acids was mainly due to aromatic rings that were in plane to the graphene sheet. The density of state (DOS) analysis showed that the interaction between graphene sheets and amino acids are non-covalent in nature. The dispersion of graphene sheets in water was due to non-covalent interaction of BSA and graphene, which in turn was because of the effect of hydrophobic amino acids containing aromatic rings and aliphatic side chains [36].

2.4.2 Effect of BSA concentration & milling time on exfoliation

X-Ray diffraction was primarily used to investigate the exfoliation of graphene. The reduction in the size of graphite flakes is caused due to the diminishing of the π- π stacked layers and is indicated by the decreasing of the (002) peak intensity. Furthermore, this demonstrates that the size of the graphite particles is reducing normal to the basal plane. Also, there is an increase in the 002 peak's full width at half maxima due to Scherrer broadening along with reduction in peak intensity [38], [39].

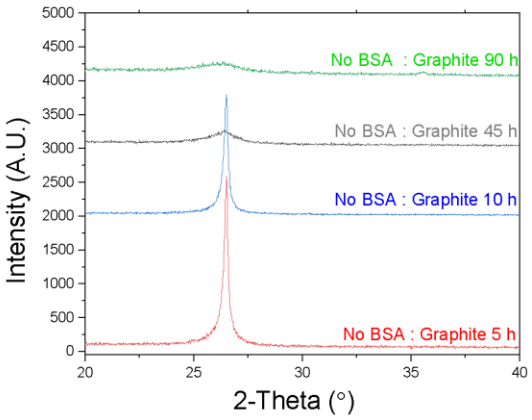

Figure 2-5 Evolution of 002 Bragg peak for varying time periods after ball milling graphite in the absence of BSA

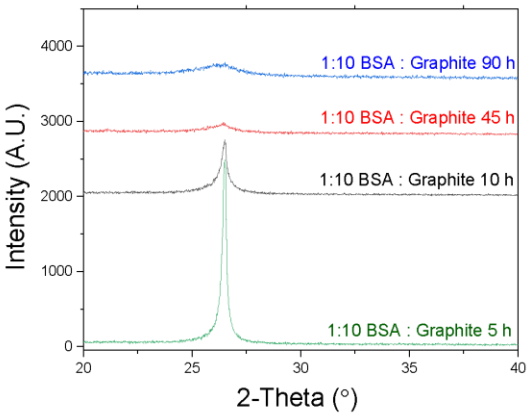

Figure 2-6 Evolution of 002 Bragg peak for varying time periods after ball milling graphite and BSA in the ratio of 1:10 respectively

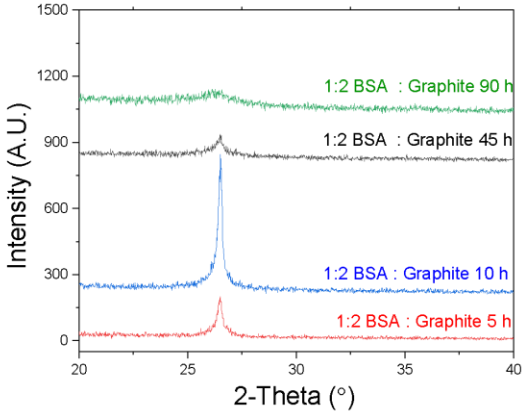

Figure 2-7 Evolution of 002 Bragg peak for varying time periods after ball milling graphite and BSA in the ratio of 1:2 respectively

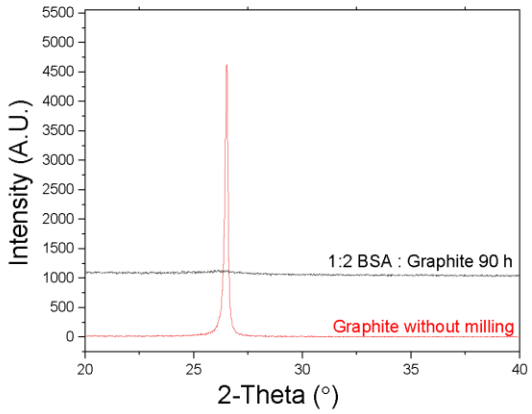

Figure 2-8 Ball milled graphene and BSA in the ratio of 1:2 respectively, compared with pure graphite

While ball-milling time was a contributor to the exfoliation of graphene sheets, it was found that ball-milling for shorter durations of time produced sharp 2θ peaks [Figure 2-5 to 2-8]. This could be attributed to the fact that graphite particles are randomly oriented which results in the flakes experiencing a combination of compressive and shear forces, which might cancel each other.

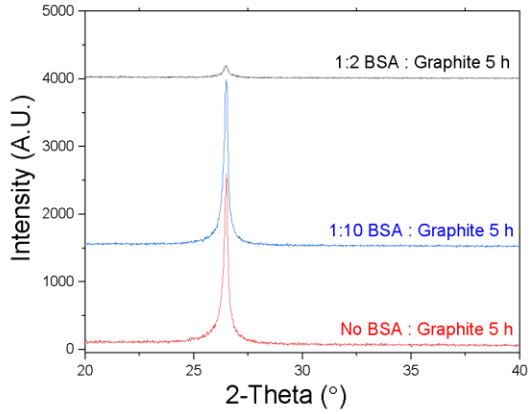

Figure 2-9 Evolution of 002 Bragg peak for varying concentrations of BSA after 5 h of ball milling

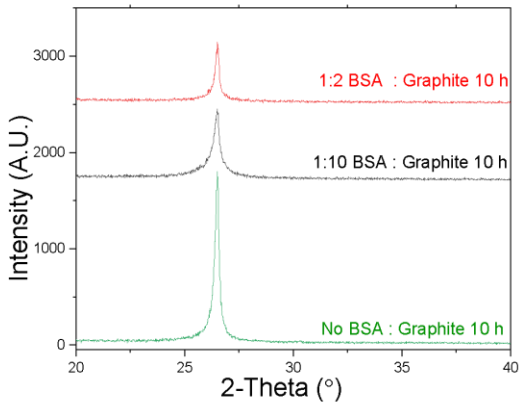

Figure 2-10 Evolution of 002 Bragg peak for varying concentrations of BSA after 10 h of ball milling

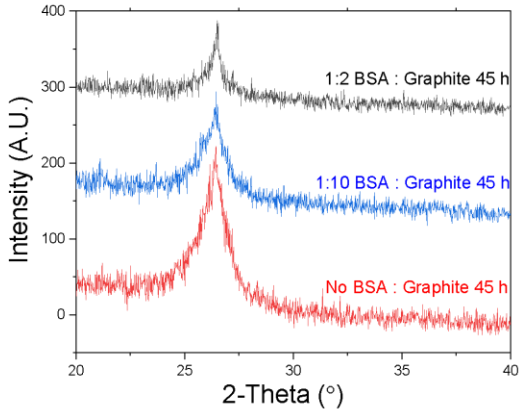

Figure 2-11 Evolution of 002 Bragg peak for varying concentrations of BSA after 45 h of ball milling

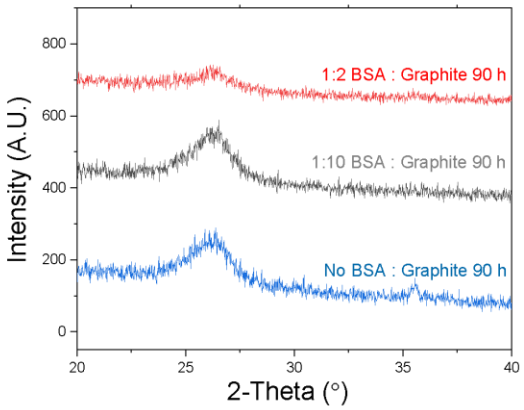

Figure 2-12 Evolution of 002 Bragg peak for varying concentrations of BSA after 90 h of ball milling

Additionally, the individual graphene layers generally restack unless there is an intercalation agent preventing it [40], [38]. It was noted that after ball-milling graphite for 90 hours in the absence of BSA, the 2θ peaks produced were broad and graphene like [Figure 2-9 to 2-12]**.** Also, this is the first time that graphene has been exfoliated in the absence of any intercalating agent by ball milling. However, the application of such prolonged times can be considered uncompetitive for industrial applications. Also, samples milled for long periods of time can get contaminated, especially from materials present in the balls as well as the milling jar. It was observed that the graphene produced after milling for 90 hours, without BSA, was magnetic, which was attributed to iron contamination from the steel jars.

Moreover, increasing the initial concentration of BSA helped expedite the separation of graphene sheets. The effect of BSA in the exfoliation of graphene is prominent for shorter milling times, although its effects are subtly visible for longer periods.

2.4.3 Optimization of milling parameters

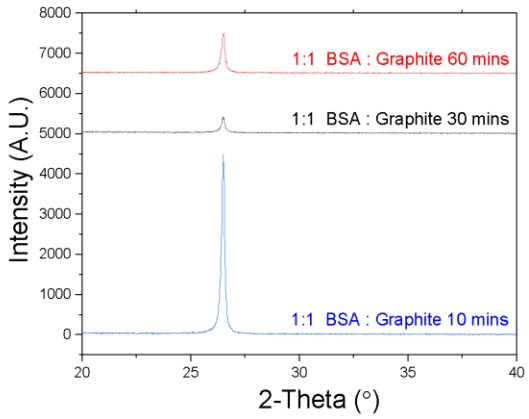

Figure 2-13 Evolution of 002 Bragg peak for 1:1 BSA : graphite after milling for short time periods

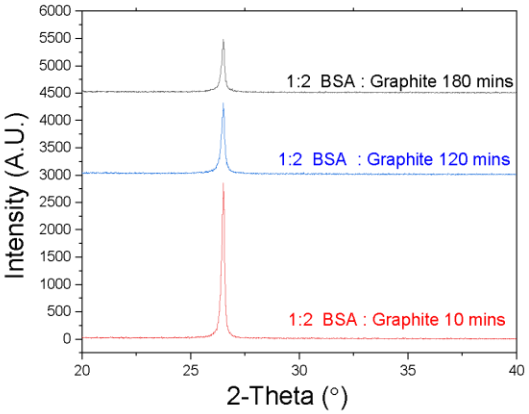

Figure 2-14 Evolution of 002 Bragg peak for 1:2 BSA : graphite after milling for short time periods

The initial experimental design of this study was to investigate the effects of specific ball milling times with increase in initial concentration of BSA. However, after noting the impactful effects of BSA in the exfoliation of graphene, the milling time was drastically cut short to further optimize the process. Milling equal concentrations of BSA and graphite for an hour gave significantly better results than those obtained after 10 hours in the absence of BSA [Figure 2-13 & 2-14].

2.4.4 Scanning Electron Microscopy Results

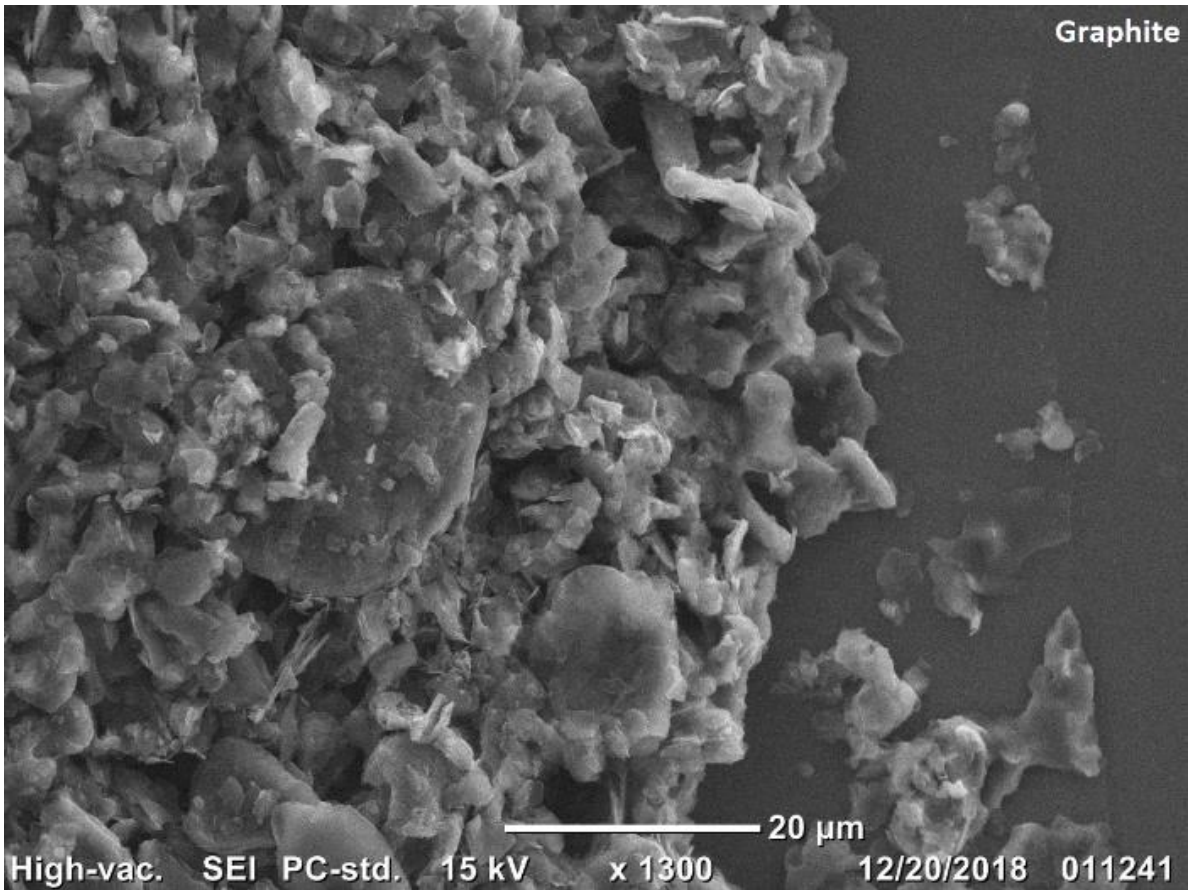

Figure 2-15 Scanning electron microscope image of graphite

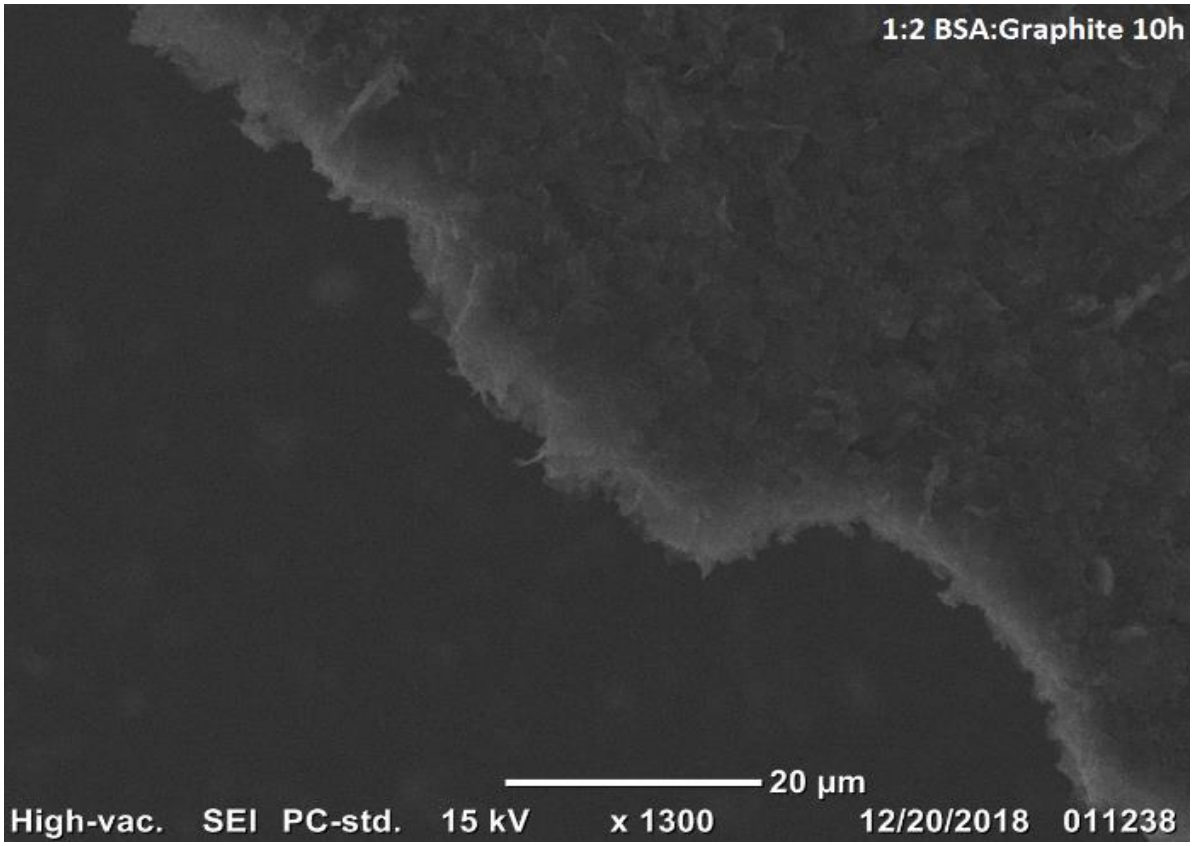

Figure 2-16 Scanning electron microscope image of graphene

Scannning Electron Microscopy (SEM) was used to perform a preliminary study on the morphology of the FLG particles and graphite flakes before and after milling. A distinct difference could be observed between the structure of graphite flakes and the milled FLG [Figure 2-15 & 2-16].

2.4.5 Transmission Electron Microscopy Results

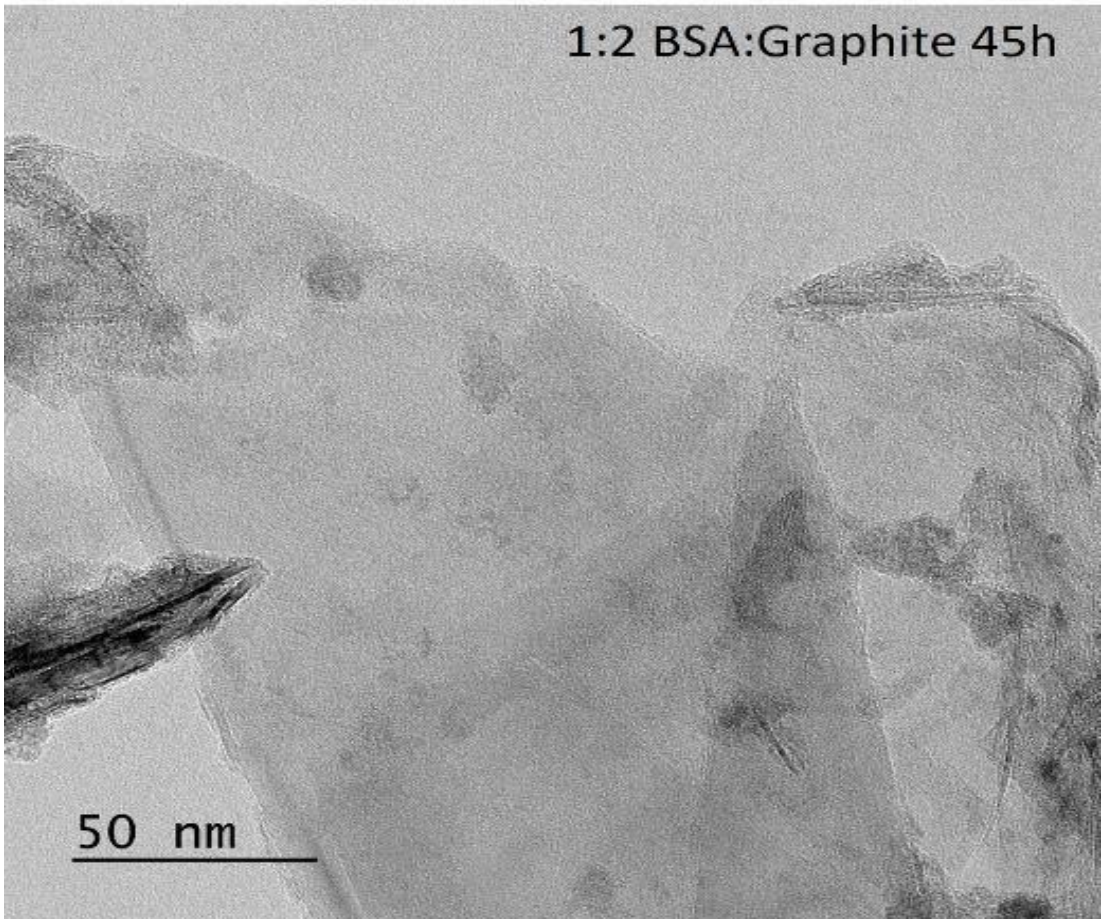

Figure 2-17 Transmission electron microscope image of 45 hour milled 1:2 BSA-graphite sample

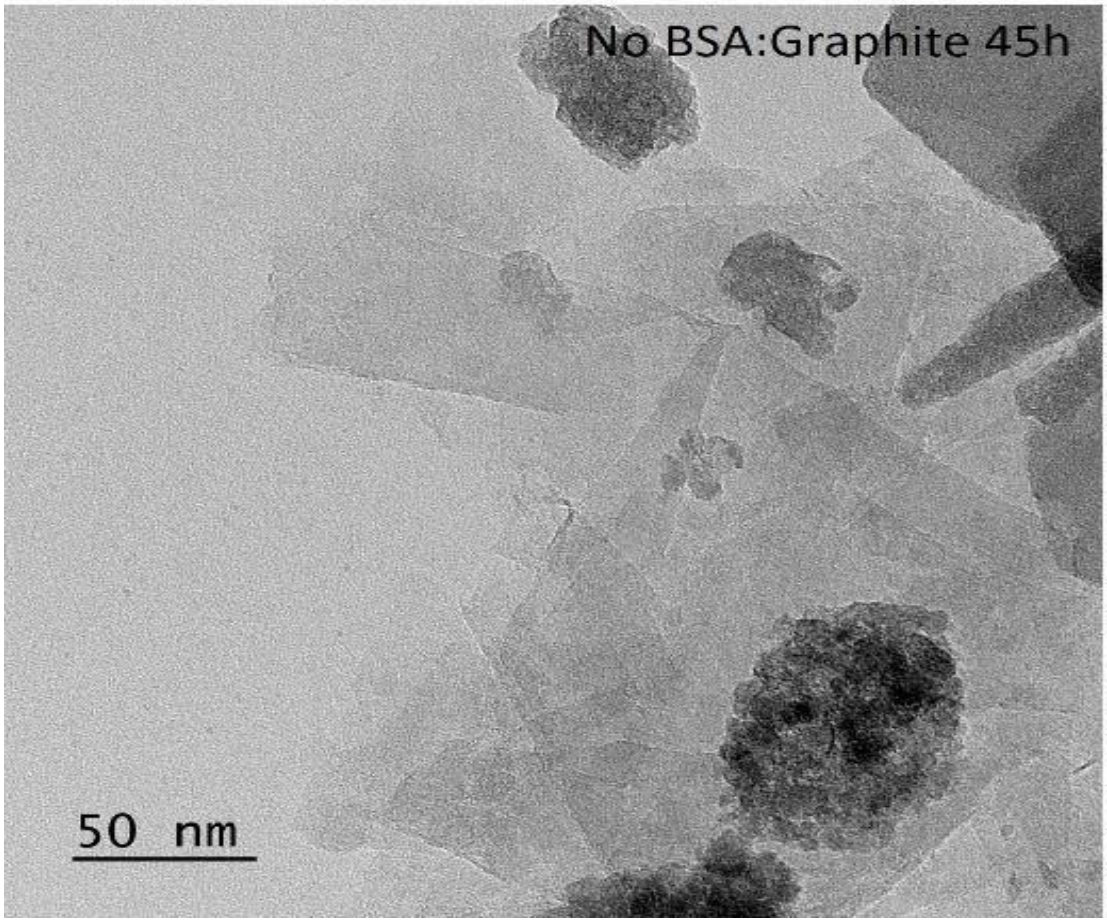

Figure 2-18 Transmission electron microscope image of 45 hour milled graphite sample (no BSA)

Transmission electron microscopy was employed to further discern the structure of the ball milled material. The FLG was in the form of folded nanosheets, however the sample containing BSA was found to contain mono-layer graphene. Moreover, it can be verified that despite the same number of milling hours, BSA-FLGs have lower number of layers than those without BSA [Figure 2-17 & 2-18].

2.4.6 Detection of disorder produced during the ball milling process

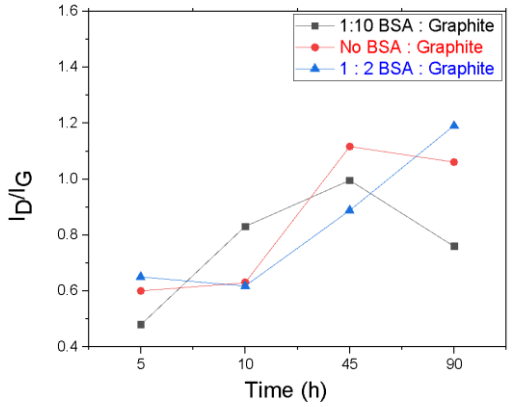

Figure 2-19 Variation in the ID/IG ratio with milling time and concentration of BSA

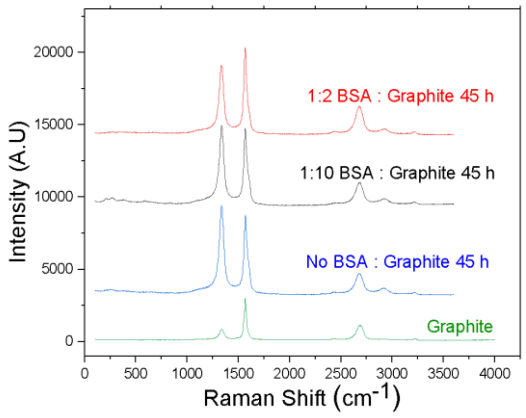

Figure 2-20 Raman spectra for graphite and graphene after 45 hours of milling

The effect of ball milling on the production of defects and graphene exfoliation was determined using Raman spectroscopy. The D and G peaks are the prominent peaks observed in the Raman spectra of carbon materials and other polyromantic hydrocarbons[41], [42], [43]. These

peaks can be observed at approximately 1360 cm^{-1} and 1560 cm^{-1} [41]. The appearance of the D peak is an indicator of defects within the material [44], [45], [46]. Ferrari *et al.* collected Raman spectra using 514.5 nm laser excitation on graphite and graphene. The G peak and the 2D band were acutely observed at approximately 1580 cm^{-1} and 2700 cm^{-1}, respectively [47], [48]. An additional peak was observed in the spectra at approximately 3250 cm^{-1} and has been referred to as the 2D' peak [47, 49].

The defects produced due to the milling process is overall directly proportional to the number of hours the process was carried out. However, no clear trend could be discerned to describe the effect of BSA on the formation of defects. The I_D/I_G, a numerical value denoting the production of defects, ranged from 0.48 to 1.19, the latter arising after grinding was performed for 90 h [Figure 2-19 & 2-20]. Gonzalez et *al.* obtained an I_D/I_G of approximately 1.8 after milling for 8 hours using glucose. However, even after milling for 90 hours using BSA, the BSA-FLG has lower defect ratios than that produced using glucose as an exfoliating agent [35]. Additionally, Pattammattel *et al.* discovered that the I_D/I_G ratios reached up to 0.6 after exfoliating graphene in the presence of BSA using the shearing force applied by a kitchen blender. It can be inferred that any application of shear force for the production of graphene tends to generate defects in the material [37].

The spectra denoting the Raman Shift for 45-hour ball milled samples shows that the relative intensity of the D band compared to the G band constantly reduces with the addition of BSA, with the exception for pristine graphite which possesses a low I_D/I_G ratio as expected. Also, the FWHM increases with milling and the addition of BSA, which is similar to the results obtained by Pattammattel *et al.* [37].

2.4.7 Integration of BSA-FLG with Astrocyte cells

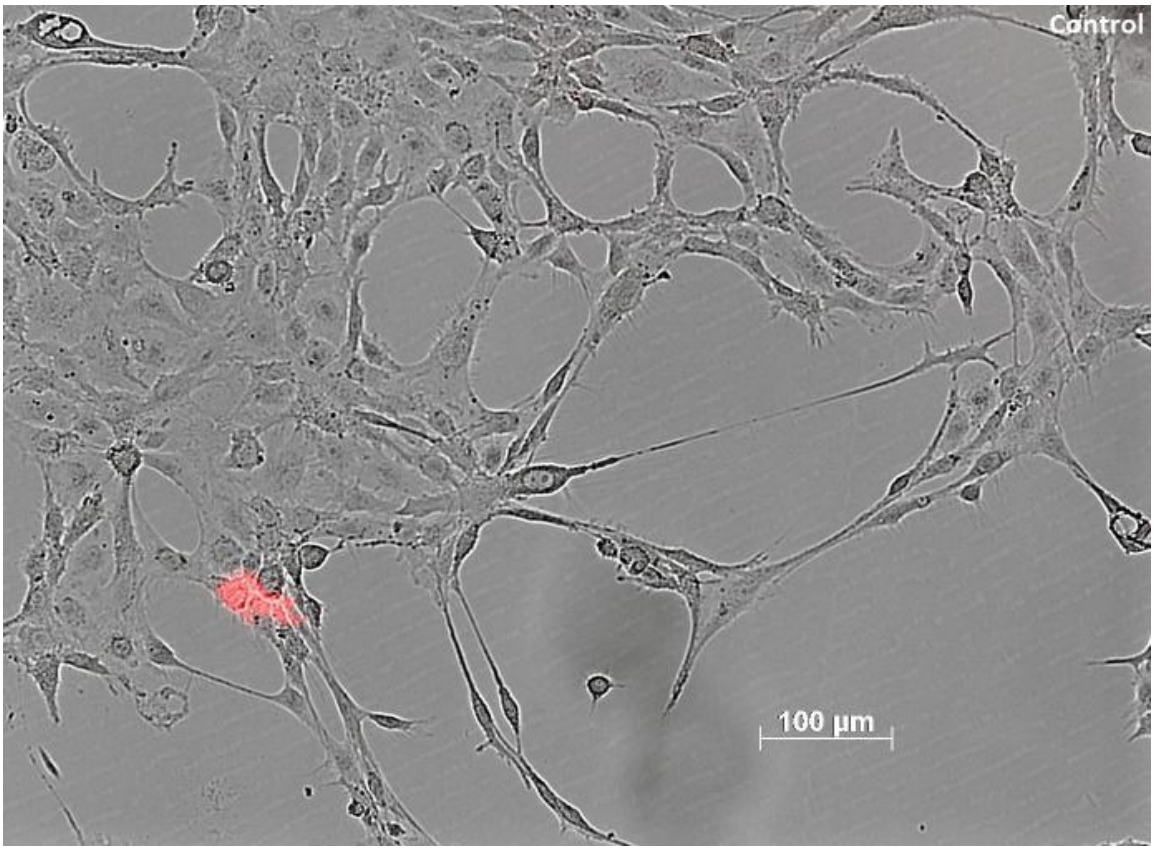

Figure 2-21 Inverted microscope image of Astrocyte cells (Control)

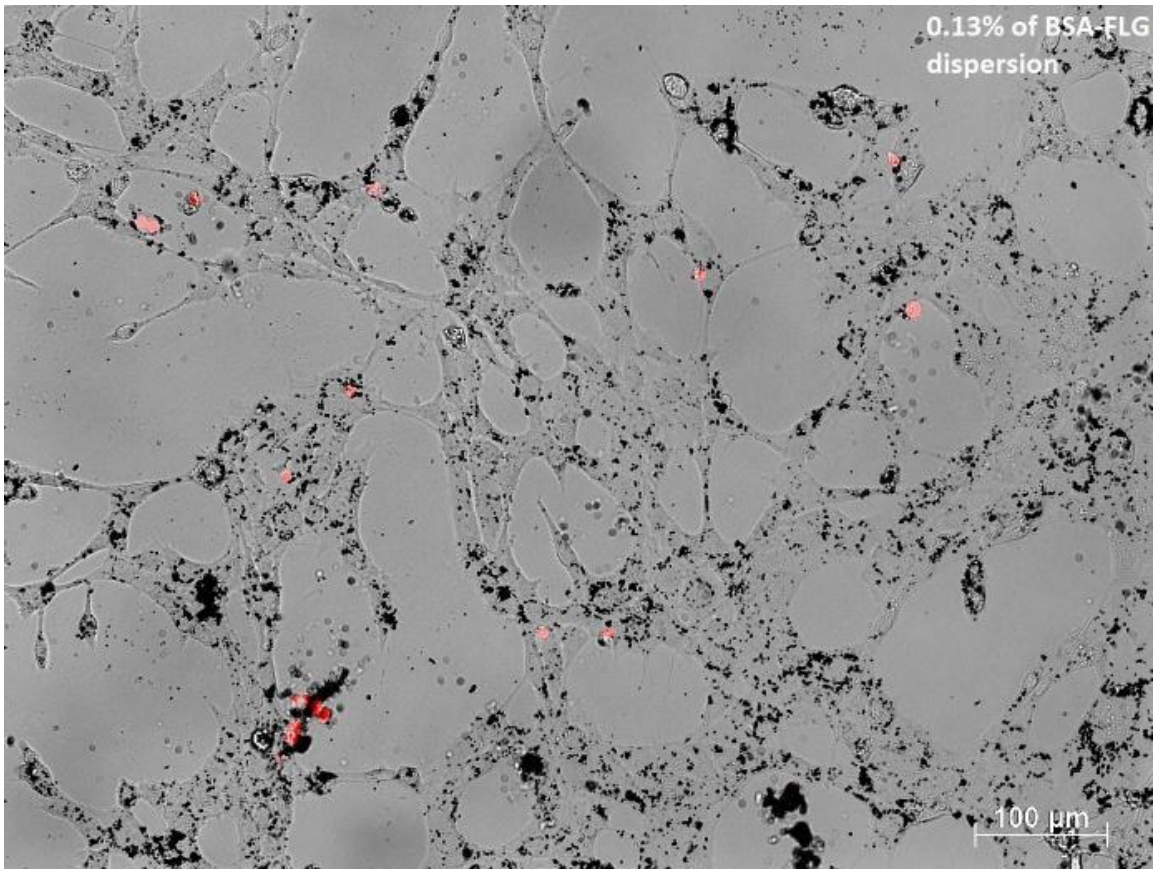

Figure 2-22 Inverted microscope image of Astrocyte cells integrated with 0.13% of BSA-FLG dispersion

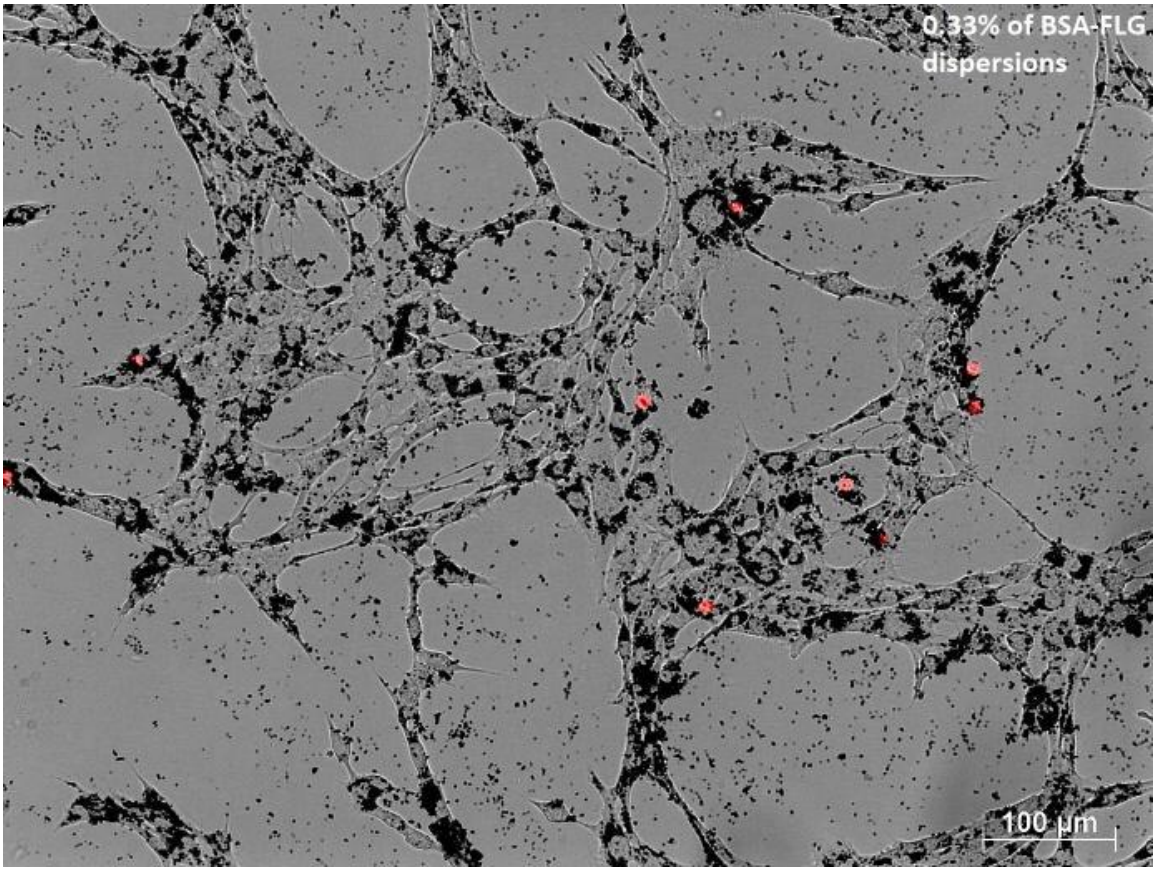

Figure 2-23 Inverted microscope image of Astrocyte cells integrated with 0.33% of BSA-FLG dispersion

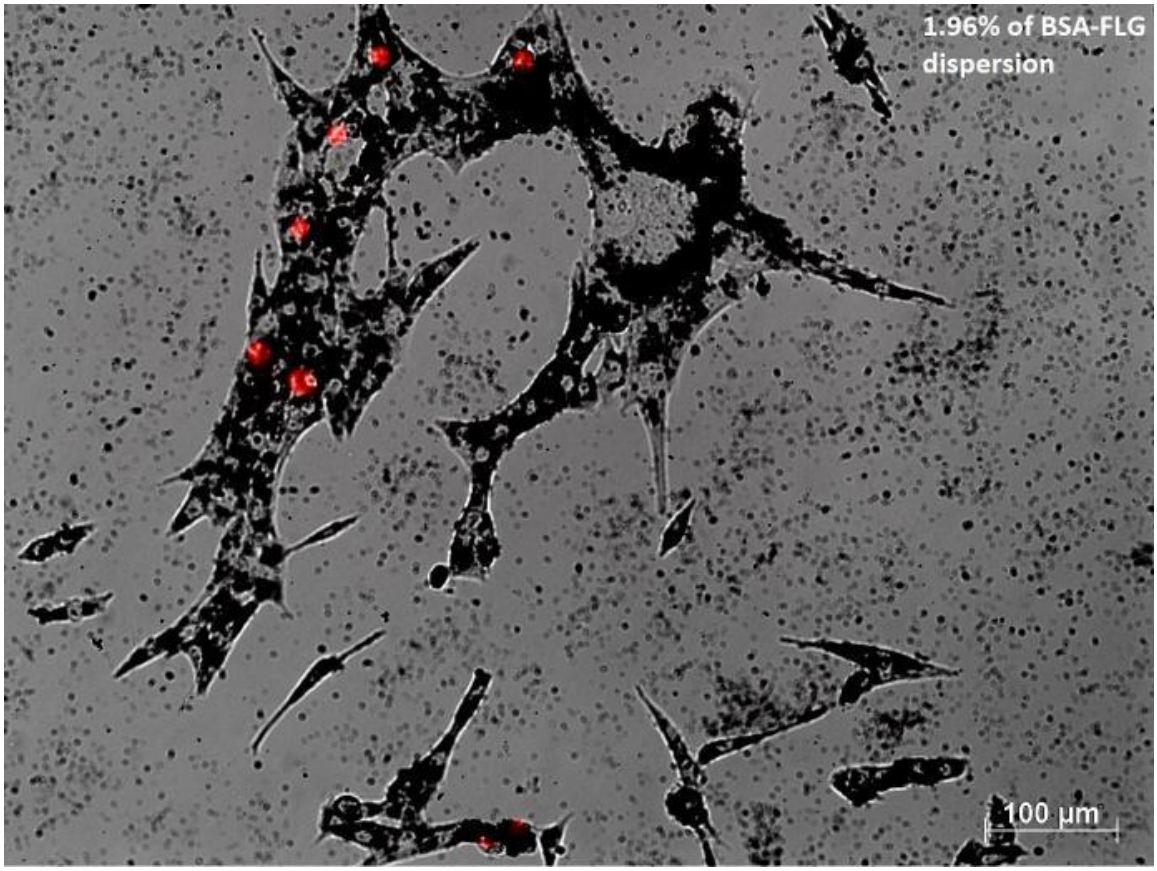

Figure 2-24 Inverted microscope image of Astrocyte cells integrated with 1.96% of BSA-FLG dispersion

Astrocytes are a type of glial cell abundantly found in the central nervous system (CNS). They perform a variety of functions including axon guidance, synaptic support, control blood brain barrier and are very responsive to CNS attacks [50]. Sasidharan *et al.* discovered that cell apoptosis occurs due to pristine graphene collecting around its membrane. This was attributed to the powerful hydrophobic interaction that pristine graphene had with the hydrophobic cellular membrane. They theorized that essential nutrients, proteins and ion channels were sealed off by pristine graphene, which leads to the formation of reactive oxygen species (ROS) stress. However, they found that hydrophilic graphene did not exhibit the

harmful traits that hydrophobic graphene possessed. They concluded that surface functionalization is one of the salient factors that mitigate the cytotoxic characteristics of pristine graphene [51]. Since the hydrophobic portion of BSA is adsorbed on graphene, the hydrophilic part interacts with water and the surrounding environment promoting a benign interaction with cells. BSA-FLG was placed in cell media with Astrocytes cells at varying concentrations, for a duration of approximately three days to experimentally study its effects on them. The optical imaging technique employed shows that at lower concentrations of BSA-FLG dispersions (~0.13%) only a small proportion of cells were affected at the locations studied. However, at higher concentrations (1.96 %) a larger number of cells died [Figure 2-21 to 2-24].

2.5 Conclusion

This paper investigates a mechano-chemical process to fabricate bio-compatible graphene. The effect of BSA on the accelerated exfoliation of graphene while producing relatively lower defects can be easily discerned. Additionally, this paper shows the production of graphene in the absence of any exfoliating agent after milling for large time periods. Preliminary investigations found that lower concentrations of BSA-functionalized graphene can be integrated with cells without inducing their death. Future work can include investigations of the optimal amount of BSA that allow high concentrations of graphene to be placed within the cell media.

2.6 Experimental

X-ray powder diffraction analysis The (PXRD) analysis was performed at room temperature using a PANalytical X'PERT diffractometer. Cu-$K_{\alpha 1}$ radiation was employed with a 0.02° 2θ step, in the 2θ range from 10° to 80°. In order to prevent the characterized sample from being exposed to oxygen and moisture, a polyimide (Kapton) film was implemented. This causes the generation of amorphous-like background between $13° \leq 2\theta \leq 20°$.

Scanning Electron Microscopy The SEM images were taken using JCM-6000 NeoScope Benchtop microscope. The magnification was kept constant at 20 μm (X1300). The samples were placed on a silicon wafer prior to it being placed within the microscope.

Transmission Electron Microscopy The TEM images were taken using a JEOL 2100 Scanning and Electron Microscope. A Gatan OneView 4K camera was used to capture images. The sample preparation included pipetting 2 μL of the aqueous FLG dispersion onto a carbon film copper grid. The excess material was removed using a filter paper and a thin film of the material was used for characterization.

Cell Imaging The pictures of cells were captured using an inverted microscope platform (Overall view Axio Observer.A1). Propidium Iodide staining was conducted to identify cell death.

Raman Spectroscopy. Raman spectra were collected using a Horiba XploRa Plus confocal Raman upright microscope equipped with a 532 nm excitation source (1.5 mW at the sample) and a Synapse EMCCD camera. A 50x air objective (Olympus, LMPlanFL) with 0.25

numerical aperture was used to collect Raman spectra in the epi-direction. The spectra were collected from 600-3300 cm^{-1} with a 600 grooves/mm grating, each spectrum corresponds to an average of 3 measurements with a 30 s acquisition time and 2 accumulations.

Acknowledgements : This work was partially supported by the Office of Naval Research Grant N000141712620 and Army Research Office Grant W911NF1710584. The authors would like to thank Marilyn McNamara, Alex Wrede, Kelli Johnston and Jingshuai Guo for their assistance in the cell culture preparations and characterization using confocal imaging. The Raman measurements were supported by the U.S. Department of Energy, Office of Basic Energy Sciences, Division of Chemical Sciences, Geosciences, and Biosciences through the Ames Laboratory. The Ames Laboratory is operated for the U.S. Department of Energy by Iowa State University under Contract No. DE-AC02-07CH11358.

2.7 References

1. Allen, M. J.; Tung, V. C.; Kaner, R. B., Honeycomb Carbon: A Review of Graphene. *Chemical Reviews* **2010,** *110* (1), 132-145.

2. Reina, A.; Jia, X.; Ho, J.; Nezich, D.; Son, H.; Bulovic, V.; Dresselhaus, M. S.; Kong, J., Large Area, Few-Layer Graphene Films on Arbitrary Substrates by Chemical Vapor Deposition. *Nano Letters* **2009,** *9* (1), 30-35.

3. Tan, R. K. L.; Reeves, S. P.; Hashemi, N.; Thomas, D. G.; Kavak, E.; Montazami, R.; Hashemi, N. N., Graphene as a flexible electrode: review of fabrication approaches. *Journal of Materials Chemistry A* **2017,** *5* (34), 17777-17803.

4. Xie, Y.; Yuan, P.; Wang, T.; Hashemi, N.; Wang, X., Switch on the high thermal conductivity of graphene paper. *Nanoscale* **2016,** *8* (40), 17581-17597.

5. Bolotin, K. I.; Sikes, K. J.; Jiang, Z.; Klima, M.; Fudenberg, G.; Hone, J.; Kim, P.; Stormer, H. L., Ultrahigh electron mobility in suspended graphene. *Solid State Communications* **2008,** *146* (9), 351-355.

6. Edwards, R. S.; Coleman, K. S., Graphene synthesis: relationship to applications. *Nanoscale* **2013,** *5* (1), 38-51.

7. Bunch, J. S.; Verbridge, S. S.; Alden, J. S.; van der Zande, A. M.; Parpia, J. M.; Craighead, H. G.; McEuen, P. L., Impermeable Atomic Membranes from Graphene Sheets. *Nano Letters* **2008,** *8* (8), 2458-2462.

8. Lee, C.; Wei, X.; Kysar, J. W.; Hone, J., Measurement of the Elastic Properties and Intrinsic Strength of Monolayer Graphene. *Science* **2008,** *321* (5887), 385-388.

9. He, S.; Liu, K.-K.; Su, S.; Yan, J.; Mao, X.; Wang, D.; He, Y.; Li, L.-J.; Song, S.; Fan, C., Graphene-Based High-Efficiency Surface-Enhanced Raman Scattering-Active Platform for Sensitive and Multiplex DNA Detection. *Analytical Chemistry* **2012,** *84* (10), 4622-4627.

10. Rastogi, S. K.; Raghavan, G.; Yang, G.; Cohen-Karni, T., Effect of Graphene on Nonneuronal and Neuronal Cell Viability and Stress. *Nano Letters* **2017,** *17* (5), 3297-3301.

11. Berger, C.; Song, Z.; Li, X.; Wu, X.; Brown, N.; Naud, C.; Mayou, D.; Li, T.; Hass, J.; Marchenkov, A. N.; Conrad, E. H.; First, P. N.; de Heer, W. A., Electronic Confinement and Coherence in Patterned Epitaxial Graphene. *Science* **2006,** *312* (5777), 1191-1196.

12. Geim, A. K.; Novoselov, K. S., The rise of graphene. *Nature Materials* **2007,** *6*, 183.

13. Thomas, D.-G.; Kavak, E.; Hashemi, N.; Montazami, R.; Hashemi, N., Synthesis of Graphene Nanosheets through Spontaneous Sodiation Process. *C* **2018,** *4* (3), 42.

14. Hernandez, Y.; Nicolosi, V.; Lotya, M.; Blighe, F. M.; Sun, Z.; De, S.; McGovern, I. T.; Holland, B.; Byrne, M.; Gun'Ko, Y. K.; Boland, J. J.; Niraj, P.; Duesberg, G.; Krishnamurthy, S.; Goodhue, R.; Hutchison, J.; Scardaci, V.; Ferrari, A. C.; Coleman, J. N., High-yield production of graphene by liquid-phase exfoliation of graphite. *Nature Nanotechnology* **2008,** *3*, 563.

15. Batzill, M., The surface science of graphene: Metal interfaces, CVD synthesis, nanoribbons, chemical modifications, and defects. *Surface Science Reports* **2012,** *67* (3), 83-115.

16. Morozov, S. V.; Novoselov, K. S.; Schedin, F.; Jiang, D.; Firsov, A. A.; Geim, A. K., Two-dimensional electron and hole gases at the surface of graphite. *Physical Review B* **2005,** *72* (20), 201401.

17. Ghosh, A.; Subrahmanyam, K. S.; Krishna, K. S.; Datta, S.; Govindaraj, A.; Pati, S. K.; Rao, C. N. R., Uptake of H2 and CO2 by Graphene. *The Journal of Physical Chemistry C* **2008,** *112* (40), 15704-15707.

18. Novoselov, K. S.; Geim, A. K.; Morozov, S. V.; Jiang, D.; Zhang, Y.; Dubonos, S. V.; Grigorieva, I. V.; Firsov, A. A., Electric Field Effect in Atomically Thin Carbon Films. *Science* **2004,** *306* (5696), 666-669.

19. Novoselov, K. S.; Jiang, D.; Schedin, F.; Booth, T. J.; Khotkevich, V. V.; Morozov, S. V.; Geim, A. K., Two-dimensional atomic crystals. *Proceedings of the National Academy of Sciences of the United States of America* **2005,** *102* (30), 10451-10453.

20. Yi, M.; Shen, Z., A review on mechanical exfoliation for the scalable production of graphene. *Journal of Materials Chemistry A* **2015,** *3* (22), 11700-11715.

21. Novoselov, K. S.; Geim, A. K.; Morozov, S. V.; Jiang, D.; Katsnelson, M. I.; Grigorieva, I. V.; Dubonos, S. V.; Firsov, A. A., Two-dimensional gas of massless Dirac fermions in graphene. *Nature* **2005,** *438*, 197.

22. Dresselhaus, M. S.; Araujo, P. T., Perspectives on the 2010 Nobel Prize in Physics for Graphene. *ACS Nano* **2010,** *4* (11), 6297-6302.

23. FLINT, E. B.; SUSLICK, K. S., The Temperature of Cavitation. *Science* **1991,** *253* (5026), 1397-1399.

24. McNamara Iii, W. B.; Didenko, Y. T.; Suslick, K. S., Sonoluminescence temperatures during multi-bubble cavitation. *Nature* **1999,** *401*, 772.

25. Suslick, K. S.; Flannigan, D. J., Inside a Collapsing Bubble: Sonoluminescence and the Conditions During Cavitation. *Annual Review of Physical Chemistry* **2008,** *59* (1), 659-683.

26. Damm, C.; Nacken, T. J.; Peukert, W., Quantitative evaluation of delamination of graphite by wet media milling. *Carbon* **2015,** *81*, 284-294.

27. Chen, Z.; Miao, H.; Wu, J.; Tang, Y.; Yang, W.; Hou, L.; Yang, F.; Tian, X.; Zhang, L.; Li, Y., Scalable Production of Hydrophilic Graphene Nanosheets via in Situ Ball-Milling-Assisted Supercritical CO2 Exfoliation. *Industrial & Engineering Chemistry Research* **2017,** *56* (24), 6939-6944.

28. Pu, N.-W.; Wang, C.-A.; Sung, Y.; Liu, Y.-M.; Ger, M.-D., Production of few-layer graphene by supercritical CO2 exfoliation of graphite. *Materials Letters* **2009,** *63* (23), 1987-1989.

29. Cazorla-Amorós, D.; Alcaniz-Monge, J.; De la Casa-Lillo, M.; Linares-Solano, A., CO2 as an adsorptive to characterize carbon molecular sieves and activated carbons. *Langmuir* **1998,** *14* (16), 4589-4596.

30. Zhu, H.; Cao, Y.; Zhang, J.; Zhang, W.; Xu, Y.; Guo, J.; Yang, W.; Liu, J., One-step preparation of graphene nanosheets via ball milling of graphite and the application in lithium-ion batteries. *Journal of materials science* **2016,** *51* (8), 3675-3683.

31. Al-Sherbini, A.-S.; Bakr, M.; Ghoneim, I.; Saad, M., Exfoliation of graphene sheets via high energy wet milling of graphite in 2-ethylhexanol and kerosene. *Journal of advanced research* **2017,** *8* (3), 209-215.

32. Zhao, W.; Fang, M.; Wu, F.; Wu, H.; Wang, L.; Chen, G., Preparation of graphene by exfoliation of graphite using wet ball milling. *Journal of Materials Chemistry* **2010,** *20* (28), 5817-5819.

33. **Safety Information - Sigma Aldrich**. https://www.sigmaaldrich.com/catalog/product/sial/227056?lang=en&region=US.

34. León, V.; Quintana, M.; Herrero, M. A.; Fierro, J. L. G.; Hoz, A. d. l.; Prato, M.; Vázquez, E., Few-layer graphenes from ball-milling of graphite with melamine. *Chemical Communications* **2011,** *47* (39), 10936-10938.

35. González, V. J.; Rodríguez, A. M.; León, V.; Frontiñán-Rubio, J.; Fierro, J. L. G.; Durán-Prado, M.; Muñoz-García, A. B.; Pavone, M.; Vázquez, E., Sweet graphene: exfoliation of graphite and preparation of glucose-graphene cocrystals through mechanochemical treatments. *Green Chemistry* **2018,** *20* (15), 3581-3592.

36. Ahadian, S.; Estili, M.; Surya, V. J.; Ramón-Azcón, J.; Liang, X.; Shiku, H.; Ramalingam, M.; Matsue, T.; Sakka, Y.; Bae, H.; Nakajima, K.; Kawazoe, Y.; Khademhosseini, A., Facile and green production of aqueous graphene dispersions for biomedical applications. *Nanoscale* **2015,** *7* (15), 6436-6443.

37. Pattammattel, A.; Kumar, C. V., Kitchen Chemistry 101: Multigram Production of High Quality Biographene in a Blender with Edible Proteins. *Advanced Functional Materials* **2015,** *25* (45), 7088-7098.

38. Abdelkader, A. M.; Kinloch, I., Mechanochemical exfoliation of 2D crystals in deep eutectic solvents. *ACS Sustainable Chemistry & Engineering* **2016,** *4* (8), 4465-4472.

39. Zhong, Y. L.; Swager, T. M., Enhanced Electrochemical Expansion of Graphite for in Situ Electrochemical Functionalization. *Journal of the American Chemical Society* **2012,** *134* (43), 17896-17899.

40. Abdelkader, A. M.; Kinloch, I. A.; Dryfe, R. A. W., High-yield electro-oxidative preparation of graphene oxide. *Chemical Communications* **2014,** *50* (61), 8402-8404.

41. Ferrari, A.; Robertson, J., Resonant Raman spectroscopy of disordered, amorphous, and diamondlike carbon. *Physical Review B* **2001,** *64* (7), 075414.

42. Castiglioni, C.; Negri, F.; Rigolio, M.; Zerbi, G., Raman activation in disordered graphites of the A 1′ symmetry forbidden k≠ 0 phonon: the origin of the D line. *The Journal of Chemical Physics* **2001,** *115* (8), 3769-3778.

43. Ferrari, A. C.; Robertson, J.; Castiglioni, C.; Tommasini, M.; Zerbi, G., Raman spectroscopy of polyconjugated molecules and materials: confinement effect in one and two dimensions. *Philosophical Transactions of the Royal Society of London. Series A: Mathematical, Physical and Engineering Sciences* **2004,** *362* (1824), 2425-2459.

44. Ferrari, A. C.; Robertson, J., Resonant Raman spectroscopy of disordered, amorphous, and diamondlike carbon. *Physical Review B* **2001,** *64* (7), 075414.

45. Thomsen, C.; Reich, S., Double Resonant Raman Scattering in Graphite. *Physical Review Letters* **2000,** *85* (24), 5214-5217.

46. Soldano, C.; Mahmood, A.; Dujardin, E., Production, properties and potential of graphene. *Carbon* **2010,** *48* (8), 2127-2150.

47. Ferrari, A. C.; Meyer, J. C.; Scardaci, V.; Casiraghi, C.; Lazzeri, M.; Mauri, F.; Piscanec, S.; Jiang, D.; Novoselov, K. S.; Roth, S.; Geim, A. K., Raman Spectrum of Graphene and Graphene Layers. *Physical Review Letters* **2006,** *97* (18), 187401.

48. Vidano, R. P.; Fischbach, D. B.; Willis, L. J.; Loehr, T. M., Observation of Raman band shifting with excitation wavelength for carbons and graphites. *Solid State Communications* **1981,** *39* (2), 341-344.

49. Ferrari, A. C., Raman spectroscopy of graphene and graphite: Disorder, electron–phonon coupling, doping and nonadiabatic effects. *Solid State Communications* **2007,** *143* (1), 47-57.

50. Sofroniew, M. V.; Vinters, H. V., Astrocytes: biology and pathology. *Acta neuropathologica* **2010,** *119* (1), 7-35.

51. Sasidharan, A.; Panchakarla, L.; Chandran, P.; Menon, D.; Nair, S.; Rao, C.; Koyakutty, M., Differential nano-bio interactions and toxicity effects of pristine versus functionalized graphene. *Nanoscale* **2011,** *3* (6), 2461-2464.

CHAPTER 3. CONCLUSIONS & FUTURE WORK

The results presented in Chapter 2 indicate that FLGs can be produced in an environmentally friendly and economical way. Additionally, it showed the significant role that milling time and the ratio of BSA to graphite played in the exfoliation of graphene. Numerical computations showing the effect of these combined factors can be performed leading to better understanding of the forces generated during the milling processes. Additionally, these computations will give a better insight on the breakdown of the proteins under the influence of milling forces alongside its effect on graphene exfoliation. Furthermore, additional factors, such as type of protein, milling processes, speeds and ball - jar materials can be systematically varied in order to further optimize the process.

The preliminary study on cell viability in the presence of BSA-FLG dispersion showed that low concentrations of BSA-functionalized graphene did not significantly affect cells, whereas higher concentrations induced cell death. However, the individual effect of concentration of BSA in BSA-FLG dispersions, on cell apoptosis was not examined. This investigation can give us a better insight into the functionalized FLG-cell interactions and potentially pave the way for a greater impact of graphene in biotechnological applications.